ELSEVIER

Effect of iron-doping on spin-state transition and ferromagnetism in $Pr_{0.5}Ca_{0.5}CoO_{3-\delta}$ cobalt oxides

X.G. Luo, X. Li, G.Y. Wang, G. Wu, X.H. Chen*

Hefei National Laboratory for Physical Science at Microscale and Department of Physics, University of Science and Technology of China, Hefei, Anhui 230026, People's Republic of China

Abstract

Resistivity and DC magnetization measurements were performed for the polycrystalline $Pr_{0.5}Ca_{0.5}Co_{1-x}Fe_xO_{3-\delta}$ ($x = 0, 0.05, 0.10$ and 0.15) samples. The as-fabricated samples exhibit ferromagnetic (FM) transition and the transition temperature increases with increasing the Fe doping level. Annealing under the high oxygen pressure induces a spin-state transition of Co ions in the *iron-free* sample and such transition is reinforced with increasing the annealing oxygen pressure, while the annealing under high oxygen pressure suppresses the ferromagnetic ordering. Contrary to the case of the *iron-free* sample, no spin-state transition is induced by the annealing under high oxygen pressure for the *Fe-doped* samples, and the ferromagnetic transition temperature is nearly independent of the annealing procedures. The enhancement of the spin-state transition in the *iron-free* sample after annealing under high oxygen pressure should be attributed to the oxygen vacancies and the reduction of the cell volume. The suppression of the spin-state transition by the Fe doping is related to the enlargement of the cell volume. The enhancement of the ferromagnetism by the Fe-doping might arise from the ferromagnetic exchange interaction between Fe^{3+} and LS Co^{4+} through oxygen atom (Fe^{3+}–O–Co^{4+}).

1. Introduction

An intriguing feature of the perovskite-related cobalt oxides is the existence of spin-state transition (SST), which can be induced by temperature, pressure, or carrier concentration. There are various spin states for trivalent (low-spin LS: $t_{2g}^6 e_g^0$; intermediate-spin IS: $t_{2g}^5 e_g^1$; high-spin HS: $t_{2g}^4 e_g^2$) and tetravalent cobalt ions (LS: $t_{2g}^5 e_g^0$; IS: $t_{2g}^4 e_g^1$; HS: $t_{2g}^3 e_g^2$). Recent experimental and theoretical investigations indicate that in hole-doped compounds the spin states are LS and the mixture of IS/LS for tetravalent and trivalent cobalt ions, respectively [1,2]. The conversion of different spin state arises from the competition between comparable the crystal-field with energy Δ_{CF} (t_{2g}–e_g splitting) and the intraatomic (Hund) exchange with energy J_{ex} in magnitude, leading to the redistribution of electrons

between the t_{2g} and e_g levels. Δ_{CF} is found to be very sensitive to the variation in the Co–O bond length ($d_{Co−O}$), so that the subtle balance between Δ_{CF} and J_{ex} may be easily disrupted by the different kind of effects such as hole-doping and chemical or external pressure [3–6]. In the simplest perovskite-type $LnCoO_3$ ($Ln = Y$, and rare earth elements), a transition from low-spin to high- or intermediate-spin was observed with increasing the temperature [1,7–10]. In another interesting oxygen-deficient cobalt oxides $LnBaCo_2O_{5+\delta}$ ($Ln = Pr$, Nd, Sm, Eu, Gd and Tb), an abrupt SST was reported as $\delta = 0.5$ [11–15]. As one knows, the electrical conduction in the perovskite-type cobalt oxides is mainly realized through the hopping itinerant e_g electrons. The metal–insulator transition (MIT) is often accompanied with a SST. A metal to insulator transition in resistivity occurs smoothly in $LaCoO_3$ as the spin-state changes around $500\,K$ [16]. In $LnBaCo_2O_{5+\delta}$ ($Ln = Pr$, Nd, Sm, Eu, Gd and Tb), an abrupt MIT takes place simultaneously as the SST occurs

*Corresponding author.

E-mail address: chenxh@ustc.edu.cn (X.H. Chen).

[11–15]. The occurrence of MIT accompanying with the SST suggests the essential role of the e_g electrons in the metallic electronic conduction.

In the present paper, we paid our attention on another cobalt oxide $Pr_{0.5}Ca_{0.5}CoO_{3-\delta}$, which was reported firstly by Tsubouchi et al. [17,18] to exhibit the simultaneous MIT and SST at low temperature. Tsubouchi et al. believe that the decrease of Co–O–Co bond angle results in a reduction of covalency and thus unstabilizes the itinerant IS state. The lattice volume contraction induced by the decrease Co–O–Co bond angle can enlarge the splitting of crystal field, which also stabilizes the LS state. As one knows, the ferromagnetic exchanges occur mainly through the e_g hopping in perovskite-type cobalt oxides. The reduction in the population of the e_g electrons has the effect of suppressing ferromagnetism, which has been demonstrated by the previous researches of using the external pressure [5,6] or chemical pressure [19,20]. Therefore, the degradation of spin state of the cobalt ions would suppress the e_g hopping and consequently the ferromagnetic interaction. Actually, Tsubouchi et al. [17,18] presented that the long ferromagnetic order does not appear down to 10 K in $Pr_{0.5}Ca_{0.5}CoO_3$ while, $Pr_{0.55}Ca_{0.45}CoO_3$, which has no SST at low temperature, exhibits the ferromagnetic transition. It seems to suggest that the SST is competitive with the ferromagnetism. Thus, if ferromagnetism is enhanced through some ion substitution, SST is expected to be suppressed. Maignan et al. proposed that the super-exchange between the high-spin Fe^{3+} and the low-spin Co^{4+} ions through the oxygen atom could be ferromagnetic [21]. In this work, we examined effect of Fe doping and annealing procedure under the high oxygen pressure (HP) on the ferromagnetism, SST, and charge transport in the polycrystalline $Pr_{0.5}Ca_{0.5}Co_{1-x}Fe_xO_{3-\delta}$ samples. The results indicate that the ferromagnetism is enhanced, while SST is suppressed by the Fe doping. On the other hand, the annealing procedures under the high oxygen pressure induce the SST in the *iron-free* sample, but do not change the ferromagnetic transition temperature in the Fe-doped samples.

2. Experimental procedures

The polycrystalline ceramic $Pr_{0.5}Ca_{0.5}Co_{1-x}Fe_xO_{3-\delta}$ samples with $x = 0, 0.05, 0.10$ and 0.15 were synthesized using the conventional solid state reaction method. They were prepared from a stoichiometric mixture of the fine powder of oxides: Pr_6O_{11}, $CaCO_3$, Co_2O_3 and Fe_2O_3. The stoichiometric mixture was ground carefully until the mixture became homogeneous. The mixtures then were calcined at 1200 °C in the flowing oxygen for 24 h. The calcined powder was reground and pressed into pellets. The pellets were sintered at 1200 °C in the flowing oxygen for 24 h and finally cooled to room temperature. Some portions of pellets for each composition were annealed at 600 °C for 48 h under the oxygen pressure of 115, 175 and 280 atm, respectively. The X-ray powder diffraction (XRD)

was recorded at room temperature using X Pert PRO X-ray diffractometer (Philips) with $CuK\alpha$ radiation ($\lambda = 1.5418$ Å). The resistivity measurements were performed using the standard AC four-probe method. The magnetic field was supplied by a superconducting magnet system (Oxford Instruments). Magnetization measurement was carried out with a superconducting quantum interference device (SQUID) magnetometer (MPMS-7XL, Quantum Design). We also determined the oxygen content of the samples using $K_2Cr_2O_7$ titration method. An appropriate amount of sample (about 30 mg) is dissolved in the mixture of vitriol and phosphate acid, then the high-valent Co ions are deoxidized to divalent ones with Fe^{2+} ions, and finally the excess Fe^{2+} ions are titrated with $K_2Cr_2O_7$ solution. The oxygen content for the as-fabricated samples with different Fe doping levels was determined as 2.930 ± 0.005. The oxygen content increases after annealing under the oxygen pressure, and changes to 2.959 ± 0.005 at 115 atm, 2.978 ± 0.003 at 175 atm and 2.990 ± 0.002 at 280 atm, respectively.

3. Experimental results

3.1. Structural characterization

In Fig. 1, the lattice parameters and the unit cell volumes of the as-fabricated $Pr_{0.5}Ca_{0.5}Co_{1-x}Fe_xO_{3-\delta}$ ($x = 0, 0.05, 0.10$ and 0.15) samples determined by the XRD patterns at room temperature are plotted against x. In the determination of the lattice parameters, the orthorhombic structural symmetry is assumed and the volume is estimated for the cell described by $\sqrt{2}a_p \times 2a_p \times \sqrt{2}a_p$ (space group *Pnma*)
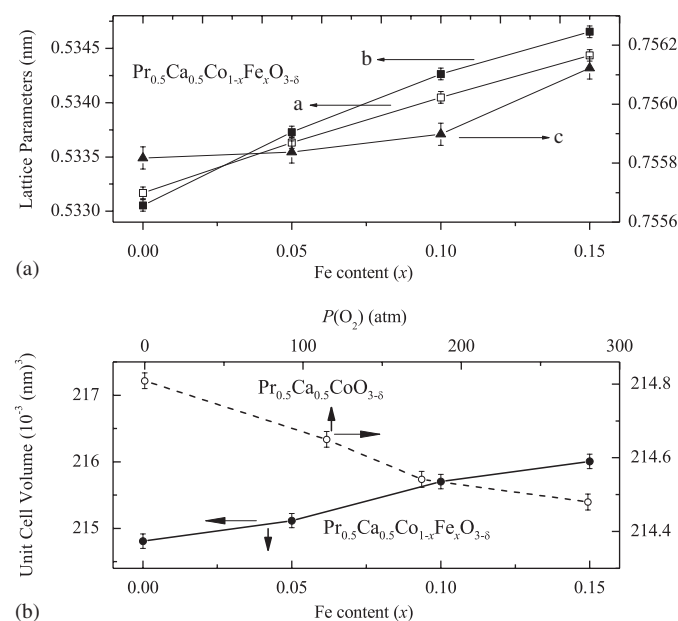

Fig. 1. The lattice parameters (a) and unit cell volume (b) variation with x for the as-fabricated $Pr_{0.5}Ca_{0.5}Co_{1-x}Fe_xO_{3-\delta}$ polycrystals. The unit cell volume a function of annealing oxygen pressure is also given in (b).

with a_p being the lattice constant of the cubic perovskite cell. Such a crystallographic structure has been used in $Pr_{1-x}Ca_xCoO_3$ system previously by other authors [17,18,22]. All the lattice parameters along three axes increase with the Fe doping and then the cell volume increases with x, consistent with the fact that ionic radius of Fe^{3+} is slightly larger than that of Co^{3+} and Co^{4+} [23,24]. The unit cell volumes of the iron-free sample is also shown in Fig. 1b with varying the annealing oxygen pressure. The volume decreases with increasing the oxygen pressure (oxygen content), similar to the results observed in $La_{0.5}Sr_{0.5}CoO_{3-\delta}$ [25].

3.2. The magnetic and transport properties for the as-fabricated samples

Fig. 2a shows the temperature dependence of the zero-field-cooled (ZFC) and field-cooled (FC) molar magnetization M at $H = 0.1$ T for the as-fabricated $Pr_{0.5}Ca_{0.5}Co_{1-x}Fe_xO_{3-\delta}$ ($x = 0, 0.05, 0.10$ and 0.15) samples. It clearly shows that all the samples undergo a ferromagnetic transition at the T_c (taken at the inflection point of the FC curve) which is enhanced from about 77 to 86 K with increasing x from 0 to 0.15. The Fe-doped samples exhibit almost the same FC M below 50 K, and their molar magnetization is much larger than that of the Fe-free sample. As shown in Fig. 2a, the magnetic moment of the Fe-free sample at 4 K is 2470 emu/mol ($\approx 0.44\mu_B/Co$), while it increases to 2950 emu/mol ($\approx 0.53\mu_B/Co$) by the Fe doping. The enhancement of the magnetic moment can be observed more obviously in the spontaneous magnetization determined from M–H loop collected at 4 K (Fig. 2b and c). The iron-free sample exhibits a much lower M_s ($= 0.51\mu_B/Co$) compared to $La_{0.5}Sr_{0.5}CoO_3$ ($M_s = 1.92\mu_B/Co$ [26]). M_s increases with increasing x, in accord with the results observed in Fig. 2a. Apparently, the Fe doping enhances the ferromagnetic interactions. The M_s ($= 0.83\mu_B$ per formula) for the sample with $x = 0.15$ is still much less than that in $La_{0.5}Sr_{0.5}CoO_3$. Such low spontaneous magnetization arises from the much smaller radius of A site ions (for the formation $ACoO_3$) in $Pr_{0.5}Ca_{0.5}CoO_{3-\delta}$ compared to $La_{0.5}Sr_{0.5}CoO_3$. The small radius of A site ions leads to short Co–O bond length and thus large crystal field. In this case, a part of the trivalent Co ions stays in LS state for $Pr_{0.5}Ca_{0.5}CoO_{3-\delta}$ even at room temperature, unlike almost all in the IS trivalent Co ions for the $La_{0.5}Sr_{0.5}CoO_3$. Such situation is very similar to $Gd_{1-x}Sr_xCoO_{3-\delta}$ we previously studied [20], where tendency to LS state of the trivalent Co ions leads to less conduction and weak ferromagnetism compared to $La_{1-x}Sr_xCoO_3$. Another marked feature that can be found in Fig. 2b is that the three Fe-doped samples have the same coercive force of 2535 Oe while the iron-free sample shows a much larger coercive force of 3475 Oe.

Fig. 3 presents the resistivity, ρ, as a function of temperature for the as-fabricated $Pr_{0.5}Ca_{0.5}Co_{1-x}Fe_xO_{3-\delta}$ ($x = 0, 0.05, 0.10$ and 0.15) samples. The resistivity grows
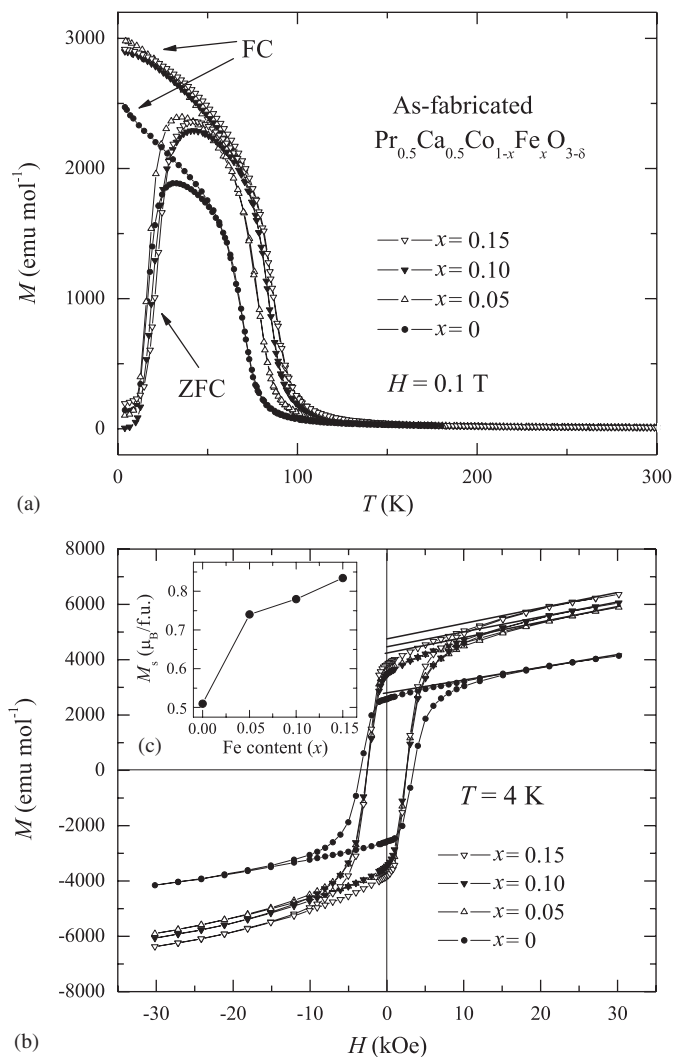

Fig. 2. (a) The temperature dependence of the molar magnetization recorded at $H = 0.1$ T for the as-fabricated $Pr_{0.5}Ca_{0.5}Co_{1-x}Fe_xO_{3-\delta}$ polycrystals. (b) The M–H loop at 4 K for these samples. The solid lines extrapolate the $M(H)$ to $H = 0$ to determined the spontaneous magnetization. (c) The spontaneous magnetization as a function of the Fe doping level.

monotonically with increasing the Fe doping level. All the samples show weak insulating behavior in the high temperatures. As indicated in the inset, the high-temperature resistivity (between 100 and 210 K for the iron-free sample) follows a 3D Mott variable-range hopping (VRH) behavior. As mentioned above, a part of trivalent Co ions is in LS state, so that the population of e_g electrons is relative small and the charge transfer from IS trivalent Co ions to LS tetravalent Co ions between clusters have to be realized through VRH format. With decreasing temperature, the resistivity for all samples exhibits the change of slope at a temperature of T_p, and a MIT occurs at T_p for the samples with $x = 0$ and 0.05. The values of T_p are 74.3, 80.2, 82.0, and 85.7 for $x = 0$, 0.05, 0.10 and 0.15, respectively. It is found that the T_p is nearly the same as the T_c. It suggests that the inflection in resistivity is induced
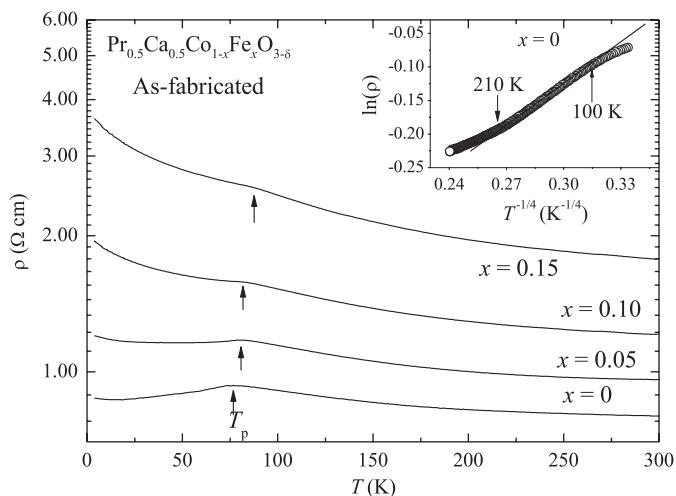
Fig. 3. The temperature dependence of the resistivity for the as-fabricated $Pr_{0.5}Ca_{0.5}Co_{1-x}Fe_xO_{3-\delta}$ polycrystals. The dashed arrows point to the T_p. The inset shows the 3D Mott VRH fit for resistivity of the iron-free sample.

Fig. 4. Resistivity collected at $H = 0$ (solid lines) and 6 T (dash lines) and magnetoresistance ($\Delta\rho/\rho$) at $H = 6$ T as the function of the temperature for the as-fabricated $Pr_{0.5}Ca_{0.5}Co_{1-x}Fe_xO_{3-\delta}$ polycrystals.

by the reduction of the spin scattering due to the ferromagnetic transition. In spite of the increase of T_p and T_c, the conductivity decreases with increasing the Fe doping level. This suggests that the enhancement of ferromagnetism cannot arise from the double exchange but other mechanisms. When a magnetic field is applied, the resistivity is suppressed dramatically at low temperatures as shown in Fig. 4. It is the typical behavior in an itinerant ferromagnet and the resistivity is reduced by magnetic field as a result of the suppression of spin-scattering. The magnetoresistance $\Delta\rho/\rho = [\rho(H) - \rho(0)]/\rho$ at $H = 6$ T is also shown in Fig. 4. Negative $\Delta\rho/\rho$ and a peak of $\Delta\rho/\rho$ around T_p are observed for all the samples. As x increases, the magnitude of the peak is reduced gradually. On the contrary, the magnitude of $\Delta\rho/\rho$ at lower temperatures is enhanced by increasing the iron content. Deduced from the increase of resistivity with the Fe doping level in the Fig. 3, it can be concluded that the Fe doping in this cobalt oxide should induce localization of carriers as well as the enhancement of ferromagnetism, probably due to the randomly distribution of the iron ions. This could be considered as the reason of the increase in magnitude of $\Delta\rho/\rho$ at 4 K.

3.3. The transport and magnetic properties for the post-annealed samples

Fig. 5a displays the temperature dependence of the resistivity for the $Pr_{0.5}Ca_{0.5}Co_{1-x}Fe_xO_{3-\delta}$ ($x = 0, 0.05, 0.10$ and 0.15) samples after annealing under the oxygen pressure of 115 atm at 600 °C. It can be found that the conductivity for the samples with $x = 0.10$ and 0.15 is enhanced, while the conductivity for the samples with $x = 0$ and 0.05 is reduced, relative to the as-fabricated samples. Especially, resistivity for the sample with $x = 0$ exhibits an abrupt increase below about 75 K. Similar abrupt jump of
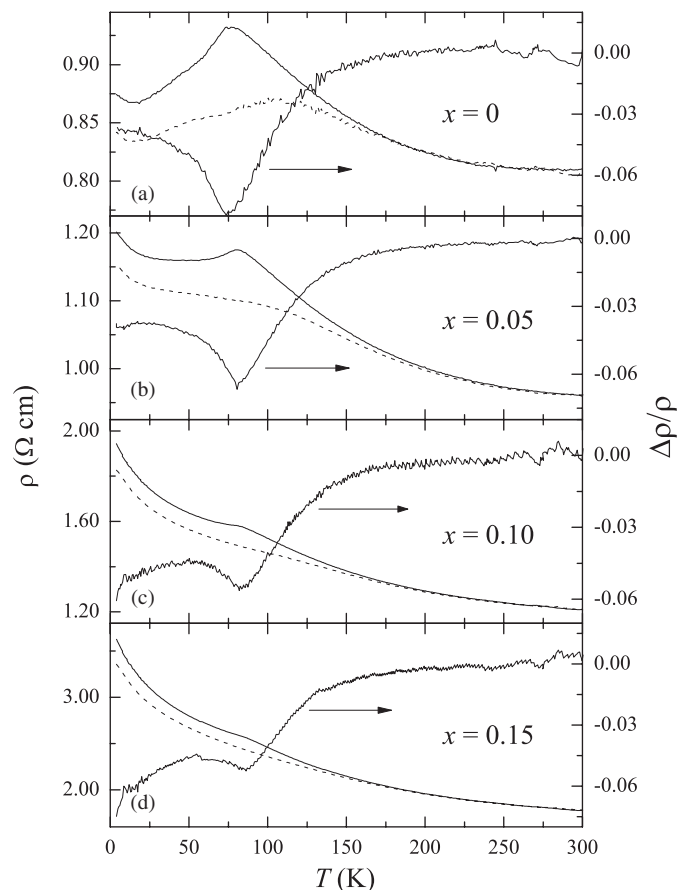
resistivity in the iron-free sample has been observed in previous reports [17,18,22], which is thought to arise from a SST, a transition from the high-temperature IS state to the low-temperature LS state. The change in resistivity from the transition point to 4 K (about 10 times) in Fig. 5a is much less than that observed in the previous reports (more than three orders in magnitude) [17,18]. Nevertheless, the sudden jump in resistivity for the iron-free sample suggests occurrence of a SST in the iron-free sample after annealing under the oxygen pressure. An annealing procedures under higher oxygen pressure should result in a larger jump in resistivity. Therefore, for the $Pr_{0.5}Ca_{0.5}Co_{1-x}Fe_xO_{3-\delta}$ ($x = 0, 0.05, 0.10$ and 0.15) samples after annealing under the oxygen pressure of 175 atm at 600 °C, their resistivity as a function of temperature is shown in Fig. 5b. The resistivity for the iron-free sample increases by more than 30 times with decreasing temperature from 70 to 4 K, much larger than that in the sample annealed under the oxygen pressure of 115 atm. This confirms that annealing procedure under the high oxygen pressure can enhance the SST. For the Fe-doped samples, resistivity of the sample with $x = 0.15$ shows very slight change, the resistivity for the samples with $x = 0.05$ and 0.10 decreases apparently
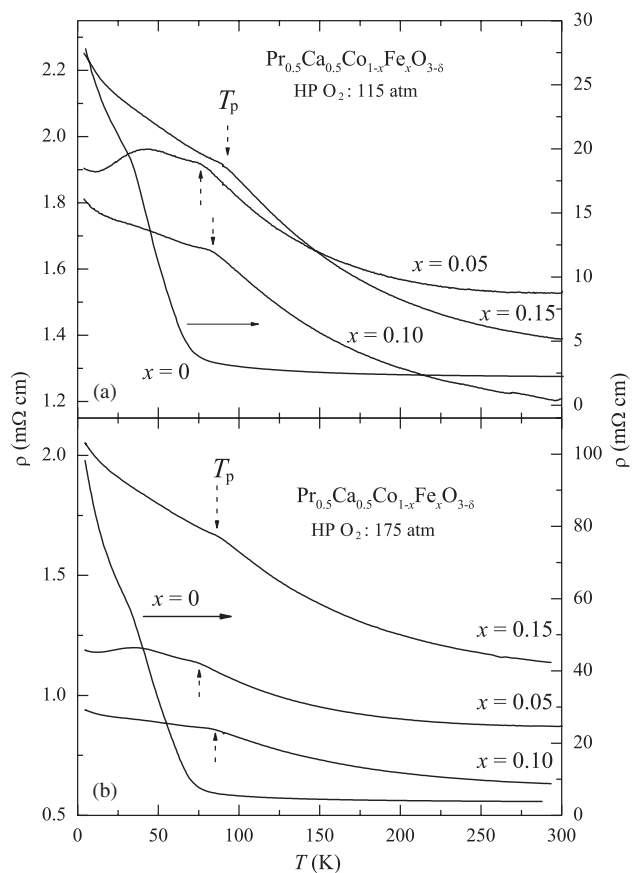
Fig. 5. (a) The temperature dependence of the resistivity for the $Pr_{0.5}Ca_{0.5}Co_{1-x}Fe_xO_{3-\delta}$ polycrystals after annealing at 600 °C and under the oxygen pressure of 115 atm. (b) The temperature dependence of the resistivity for the $Pr_{0.5}Ca_{0.5}Co_{1-x}Fe_xO_{3-\delta}$ polycrystals after annealing at 600 °C for 48 h under the oxygen pressure of 175 atm. The dashed arrows point to the T_p.

Fig. 6. The temperature dependence of the molar magnetization recorded at $H = 0.1$ T for the $Pr_{0.5}Ca_{0.5}Co_{1-x}Fe_xO_{3-\delta}$ polycrystals after annealing at 600 °C for 48 h under the oxygen pressure of 175 atm. (b) M–H loops at 4 K for these samples. The solid lines extrapolate the $M(H)$ to $H = 0$ to determined the spontaneous magnetization. (c) The spontaneous magnetization as a function of the Fe doping level.

relative to the samples annealing under the oxygen pressure of 115 atm. The temperature-dependent behavior is almost unchanged. A strange thing can be found that the temperature corresponding to the inflection of the resistivity (T_p) remains unchanged with the annealing conditions. This suggests that the ferromagnetic transition temperature for the Fe-doped samples is independent of the variation of annealing conditions.

Although the SST has been manifested apparently in the resistivity behavior in the iron-free sample after annealing under the oxygen pressure of 175 atm, Fig. 6a shows that there is still no rapid drop in magnetization around the SST temperature as observed in previous reports [17,18]. Nevertheless, the magnetization at 1000 Oe for the iron-free sample after annealing decreases apparently compared to that shown in Fig. 2a, indicating that the magnetic moment per cobalt ($0.24\mu_B$/Co at 4 K) decreases dramatically. This indicates that the SST occurs but partially. The Fe-doped samples still behave as a good ferromagnet with the same T_c as that in Fig. 2a. This is consistent with the results (T_p) indicated by resistivity. However, one should note that the magnetization at 4 K increases for the samples
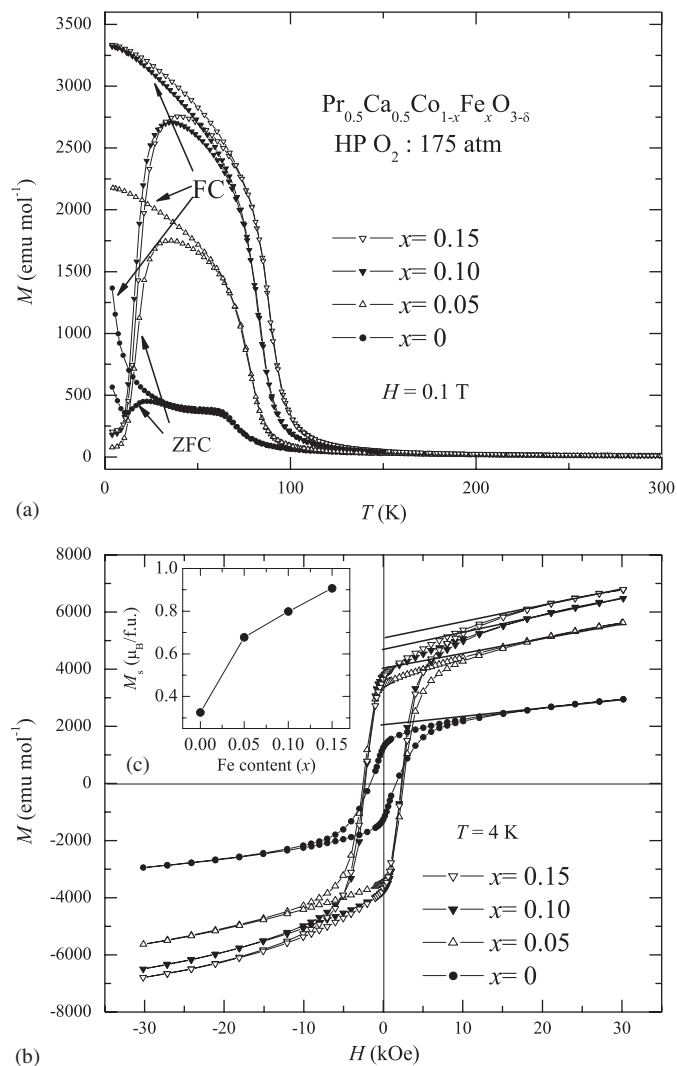
with $x = 0.10$ and 0.15 after annealing compared to the as-fabricated samples, on the contrary, the $M(T)$ for the sample with $x = 0.05$ decreases. This suggests that the degradation of the spin state in the sample with $x = 0.05$ is partly induced by annealing procedure under the high oxygen pressure. Therefore, one can observe that, similar to the iron-free sample, the resistivity of the sample with $x = 0.05$ becomes larger than that of the sample with $x = 0.10$ after annealing under the high oxygen pressure (see Fig. 5a, b). The M–H loops collected at 4 K for these four samples are shown in Fig. 6b. The enhancement of M_s with increasing Fe doping level is observed (see the inset in Fig. 6c), similar to the results in Fig. 2b and c. Much lower M_s ($0.33\mu_B$) at 4 K is obtained in Fig. 6c for the iron-free sample than that in Fig. 2c ($M_s = 0.51\mu_B$), evidencing the degradation of spin state of cobalt ions and consistent with
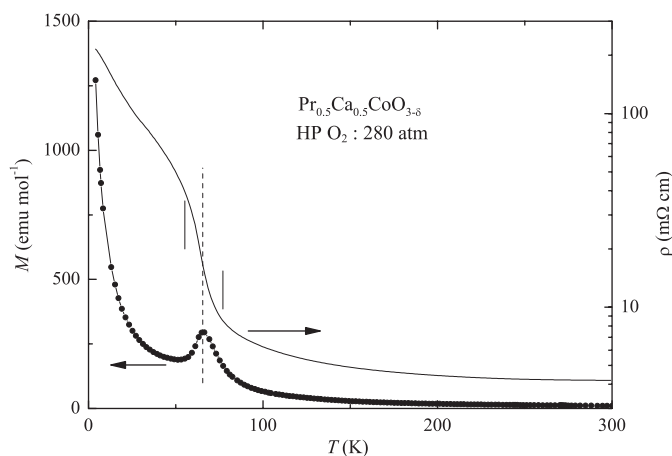
Fig. 7. The FC molar magnetization recorded at $H = 0.1$ T and the resistivity at zero field as the function temperature for the $Pr_{0.5}Ca_{0.5}CoO_{3-\delta}$ polycrystals after annealing at $600\,^\circ$C and under the oxygen pressure of 280 atm.

Fig. 8. (a) The FC molar magnetization at $H = 0.1$ T as the function temperature for the $Pr_{0.5}Ca_{0.5}CoO_{3-\delta}$ polycrystals obtained through different conditions. (b) The temperature dependence of the FC molar magnetization at $H = 0.1$ T for the as-fabricated and the annealed $Pr_{0.5}Ca_{0.5}Co_{0.95}Fe_{0.05}O_{3-\delta}$.

the results in Fig. 5. The M_s in the sample with $x = 0.15$ reaches $0.91\mu_B$, still much lower than that in $La_{0.5}Sr_{0.5}CoO_3$. It is strange that the three Fe-doped samples exhibits the same coercive force of 2410 Oe, similar to that observed in the as-fabricated samples but slightly less. The iron-free sample shows a smaller coercive force than those observed in the Fe-doped samples.

In attempt to obtain the iron-free sample with an abrupt drop in $M(T)$ at the SST temperature as observed in literatures [17,18], further annealing procedure under the oxygen pressure of 280 atm was performed. Fig. 7 shows the FC magnetization at $H = 0.1$ T and the resistivity at zero field as the function of temperature. Larger enhancement in magnitude of resistivity from 75 to 4 K is obtained compared to Fig. 5a and b, at the same time, a cusp can be observed in $M(T)$ curve at 66 K, corresponding to midpoint of the sharp increase of resistivity. Therefore, it can be concluded that annealing under the high oxygen pressure indeed promotes the SST in the iron-free sample.

4. Discussions

A most intriguing result in the present work is the enhancement of the SST by the annealing procedure under the high oxygen pressure in the iron-free sample. For the as-fabricated iron-free sample, there is no obvious indication for a SST, while after annealing under the oxygen pressure of 115 and 175 atm, the resistivity exhibits sharp MIT below 70 K, which is considered to be associated with a SST, and at the same time, the magnetization at low temperature is reduced dramatically (see Fig. 8a). After annealing under the oxygen pressure of 280 atm, a clear SST similar to that reported by other authors [17,18] is observed in the $M(T)$ curve. We have demonstrated in Section 2 that the oxygen content is enhanced with increasing the oxygen pressure in the annealing procedures. Two possibilities can be taken into account for interpreting
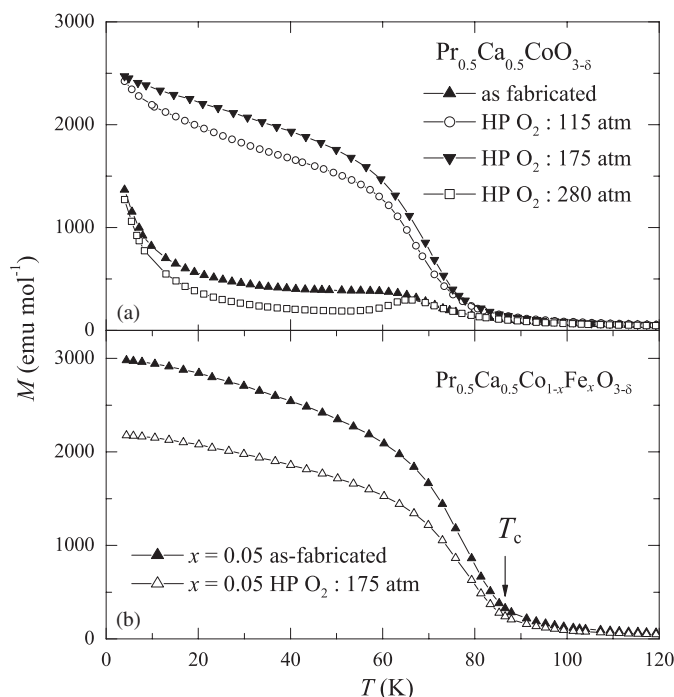
the variation of SST with the change of oxygen content. Locally, because the crystal field is weekened for the existence of oxygen vacancy, IS cobalt ions can be stabilized around oxygen vacancies. This will consequentially tend to destroy the occurrence of SST. The globally structural effects of the oxygen vacancy should be considered as another factor. Fig. 1 shows that the cell volume decreases with increasing the oxygen content in the iron-free samples. It is to say that the existence of oxygen vacancy enlarges the cell volume and then reduces the crystal field. This also favors to stabilize an IS state. In a word, SST occurs in an oxygen-stoichiometric compound and deviation of the oxygen stoichiometry tends to stabilize the IS state.

It is apparent that the Fe doping in $Pr_{0.5}Ca_{0.5}CoO_{3-\delta}$ suppresses the SST. Even after annealing under the oxygen pressure of 175 atm, clear ferromagnetic transition is observed in the sample with $x = 0.05$. This suggests that the Fe doping destroys SST. The stronger expansion of the unit cell volume with the Fe doping is observed (see Fig. 1), relative to that induced by the oxygen vacancy. Stronger effect of the Fe doping on the crystal field should be obtained than the oxygen vacancy. Therefore, the destroy of SST by the Fe doping arises from the enhancement of the crystal field by the enlargement of the cell volume. There seems to be a critical crystal field for sharp SST in $Pr_{0.5}Ca_{0.5}CoO_{3-\delta}$ system, inferred from the effect of the oxygen vacancy and the Fe doping. Slight increase of cell volume (crystal field) has dramatic effect on the SST. The

high-pressure experiment on the SST in $Pr_{1-x}Ca_xCoO_{3-\delta}$ by Fujita et al. may also illuminate this point of view. In their experiment, high pressure can induce SST in $Pr_{0.6}Ca_{0.4}CoO_{3-\delta}$, which exhibits no SST at atmosphere pressure [22].

Another interesting result induced by the Fe doping is the enhancement of ferromagnetism. As discussed above, an apparent result of the Fe doping is the suppression of the SST. So a possible candidate responsible for the enhancement of the ferromagnetism may be the enhancement of spin state of Co ions. However, Fig. 11b indicates that although the magnetization for the sample with $x = 0.05$ decreases with increasing the annealing oxygen pressure, indicative of the existence of a partly induced degradation of the spin state in this sample, the T_c remains unchanged before and after annealing. For the samples with $x = 0.10$ and 0.15 the magnetization increases with increasing the annealing oxygen pressure, but the T_c also remains unchanged before and after annealing (see Figs. 2 and 8). Therefore, it suggests that the rise of spin state as a result of the Fe doping could not be the reason of the enhancement of ferromagnetism. The enhancement of the ferromagnetism could arise from the ferromagnetic interaction around doped iron ions. According to the studies of Mössbauer spectrum in the Fe-doped $TbBaCo_2O_{5.5}$ and $La_{1-x}Sr_xCoO_3$ [28–30], the iron ions have the formation of Fe^{3+} with high-spin $t_{2g}^3 e_g^2$ electronic configuration. If we assume the same state of iron ions also exists in the present compositions, the ferromagnetic superexchange between Fe^{3+}–O–Co^{4+} in the LS Co^{4+} ions could be expected [21]. Actually, according to Goodenough–Kanamori rules, superexchange interactions through $Fe^{3+}-O-Co^{4+}(LS)$ would indeed be ferromagnetic. Because such interaction can be only present within a cluster about a Fe atom, oxygen vacancy should have little effect on T_c.

5. Conclusion

In summary, a detailed study of the magnetic and transport properties in $Pr_{0.5}Ca_{0.5}Co_{1-x}Fe_xO_{3-\delta}$ ($x = 0$, $0.05, 0.10$ and 0.15) polycrystalline bulks has been done. Although no apparent structural change is associated with the Fe doping, ferromagnetism is systematically enhanced while conductivity is suppressed for the as-fabricated samples. Annealing under high-pressure oxygen induces a SST in the iron-free sample, and the SST become more obvious with increasing the oxygen pressure. Fe doping suppresses the SST and enhances the ferromagnetic transition. The SST induced by annealing under high oxygen pressure in the *iron-free* sample is attributed to the reduction of the cell volume and oxygen vacancies as a result of the enhancement of oxygen content. The enlargement of the cell volume induced by the Fe doping is considered to lead to the suppression of SST in the Fe-doped samples. The existence of possible ferromagnetic superexchange between $Fe^{3+}-O-Co^{4+}$ is taken into account to understand the enhancement of ferromagnetism by the Fe doping.

References

[1] S. Yamaguchi, Y. Okimoto, Y. Tokura, Phys. Rev. B 54 (1996) R11022.
[2] N.N. Loshkareva, E.A. Gan'shina, B.I. Belevtsev, Y.P. Sukhorukov, E.V. Mostovshchikova, A.N. Vinogradov, V.B. Krasovitsky, I.N. Chukanova, Phys. Rev. B 68 (2003) 024413 and the references therein.
[3] K. Asai, O. Yokokura, M. Suzuki, T. Naka, T. Matsumoto, H. Takahashi, N. Mori, K. Kohn, J. Phys. Soc. Jpn. 66 (1997) 967; K. Asai, A. Yoneda, O. Yokokura, J.M. Tranquada, G. Shirane, K. Kohn, J. Phys. Soc. Jpn. 67 (1998) 290.
[4] T. Vogt, J.A. Hriljac, N.C. Hyatt, P. Woodward, Phys. Rev. B 67 (2003) 140401.
[5] R. Lengsdorf, M. Ait-Tahar, S.S. Saxena, M. Ellerby, D.I. Khomskii, H. Micklitz, T. Lorenz, M.M. Abd-Elmeguid, Phys. Rev. B 69 (2004) 140403.
[6] I. Fita, R. Szymczak, R. Puzniak, I.O. Troyanchuk, J. Fink-Finowicki, Ya.M. Mukovskii, V.N. Varyukhin, H. Szymczak, Phys. Rev. B 71 (2005) 214404.
[7] L. Sudheendra, M.M. Seikh, A.R. Raju, C. Narayana, Chem. Phys. Lett. 340 (2001) 275.
[8] J. Hejtmánek, Z. Jirák, K. Knížek, M. Maryško, M. Veverka, H. Fujishiro, J. Magn. Magn. Mater. 272–276 (2004) E283.
[9] J.Q. Yan, J.S. Zhou, J.B. Goodenough, Phys. Rev. B 69 (2004) 134409.
[10] K. Knížek, Z. Jirák, J. Hejtmánek, M. Veverka, M. Marysko, G. Maris, T.T.M. Palstra, cond-mat/0503104, 2005.
[11] N.V. Kasper, I.O. Troyanchuk, D.D. Khalyavin, N. Hamad, L. Haupt, P. Frobel, K. Barner, E. Gmelin, Q. Huang, J.W. Lynn, Phys. Status Solidi B 215 (1999) 697.
[12] Y. Moritomo, T. Akimoto, M. Takeo, A. Machida, E. Nishibori, M. Takata, M. Sakata, K. Ohoyama, A. Nakamura, Phys. Rev. B 61 (2000) R13325–R13328.
[13] D. Akahoshi, Y. Ueda, J. Solid State Chem. 156 (2001) 355.
[14] C. Frontera, J.L. Garcia-Munoz, A. Llobet, M.A.G. Aranda, Phys. Rev. B 65 (2002) 180405.
[15] C. Frontera, J.L. Garcia-Munoz, A. Llobet, M.A.G. Aranda, J. Rodriguez-Carvajal, M. Respaud, J.M. Broto, B. Raquet, H. Rakoto, M. Goiran, J. Magn. Magn. Mater. 242–245 (2002) 751.
[16] M.A. Senaris-Rodriguez, J.B. Goodenough, J. Solid State Chem. 116 (1995) 224.
[17] S. Tsubouchi, T. Kyômen, M. Itoh, P. Ganguly, M. Oguni, Y. Shimojo, Y. Morii, Y. Yoshii, Phys. Rev. B 66 (2002) 052418.
[18] S. Tsubouchi, T. Kyômen, M. Itoh, Phys. Rev. B 69 (2004) 144406.
[19] M. Kriener, C. Zobel, A. Reichl, J. Baier, M. Cwik, K. Berggold, H. Kierspel, O. Zabara, A. Freimuth, T. Lorenz, Phys. Rev. B 69 (2004) 094417.
[20] X.G. Luo, H. Li, X.H. Chen, Y.M. Xiong, G.Y. Wang, C.H. Wang, W.J. Miao, X. Li, Chem. Mater. 18 (2006) 1029.
[21] A. Maignan, C. Martin, N. Nguyen, B. Raveau, Solid State Sci. 3 (2001) 57.
[22] T. Fujita, S. Kawabata, M. Sato, K. Kakurai, M. Hedo, Y. Uwatoko, cond-mat/0502631, unpublished.
[23] R.D. Shannon, Acta Crystallogr. A 32 (1976) 751.
[24] R.D. Shannon, C.T. Prewitt, Acta Crystallogr. B 25 (1969) 925.

[25] R.P. Haggerty, R. Seshadri, J. Phys.: Condens. Matter 16 (2004) 6477.

[26] J. Wu, C. Leighton, Phys. Rev. B 67 (2003) 174408.

[28] M. Kopcewicz, D.D. Khalyavin, I.O. Troyanchuk, H. Szymczak, R. Szymczak, D.J. Logvinovich, E.N. Naumovich, J. Appl. Phys. 93 (2003) 479.

[29] Á. Cziráki, I. Geröcs, M. Köteles, A. Gábris, L. Pogány, I. Bakonyi, Z. Klencsár, A. Vértes, S.K. De, A. Barman, M. Ghosh, S. Biswas, S. Chatterjee, B. Arnold, H.D. Bauer, K. Wetzig, C. Ulhaq-Bouillet, V. Pierron-Bohnes, Eur. Phys. J. B 21 (2001) 521.

[30] Z. Homonnay, E. Kuzmann, Z. Nemeth, Z. Klencsar, S.I. Nagy, A. Vertes, Ceramics-Silikaty 48 (2004) 197.